Desalination and Water Treatment
www.deswater.com

doi: 10.1080/19443994.2015.1087344

57 (2016) 18144–18156
August

Taylor & Francis
Taylor & Francis Group

Preparation and evaluation of hydrogel composites based on starch-*g*-PNaMA/eggshell particles as dye biosorbent

Hadi Bakhshi[a,*], Atefeh Darvishi[b]

[a]*Department of Chemical and Petroleum Engineering, Sharif University of Technology, P.O. Box 11365-11155, Tehran, Iran, Tel. +98 21 66166452; emails: hadibakhshi@yahoo.com, hbakhshi@che.sharif.edu*
[b]*Young Researcher Club, Islamic Azad University, Karaj Branch, Karaj, Iran, email: darvishi.chem@yahoo.com*

Received 29 June 2015; Accepted 22 August 2015

ABSTRACT

In this study, eggshell (ES) particles as an available and low-cost waste material were used for preparing hydrogel composites as dye biosorbents. For this purpose, hydrogel composites were prepared through free-radical graft copolymerization of wheat starch and sodium methacrylate (NaMA) in the presence of different contents of ES particles with various size ranges. FTIR spectroscopy confirmed graft copolymerization of NaMA moieties onto starch backbone besides the combination of ES particles with the starch-*g*-PNaMA matrix. The gel content values were high (>99%), which showed proper graft efficiency for hydrogel composites. Incorporation of ES particles into hydrogel matrix resulted in faster water absorption at initial stage and lower equilibrium water absorption capacity. Addition of 60% ES particles into starch-*g*-PNaMA provided a cost-effective adsorbent with similar CV adsorption capacity compared to unfilled hydrogel, while MB removal was slightly decreased. The dye adsorption by hydrogel composites followed the pseudo-second-order kinetics, indicating that chemical sorption is the rate-limiting step.

Keywords: Starch; Poly(sodium methacrylate); Eggshell particles; Hydrogel composite; Dye biosorbent, adsorption kinetics

1. Introduction

Pollutants such as heavy metals, dyestuffs, and volatile organic compounds are found in wastewaters. These materials are carcinogenic and pose serious hazards to living organisms. Therefore, it is necessary to eliminate or reduce them from wastewaters before they are discharged. Dyestuffs are being removed from wastewaters by biological and physicochemical methods such as chemical precipitation, ion-exchange, adsorption, membrane filtration, coagulation-flocculation, flotation, and electrochemical processes [1]. Among these methods, adsorption technique has been widely studied in recent years on account of inexpensiveness, simplicity of design, ease of operation, availability, and ability to absorb dyes at more concentrations [1,2]. In this relation, various adsorbents such as activated carbon [2,3], chitosan [4,5], and clay [6,7] have been used.

During past two decades, polymeric hydrogels have been considered as adsorbents for the removal of pollutants from wastewaters [8,9]. Different functional

*Corresponding author.

groups such as carboxylic acid, amine, hydroxyl, and sulfonic acid have been tailored on the structure of hydrogels to improve their absorbability [9,10]. Due to hydrophilicity and high adsorption rate and capacity, hydrogels can be used as fast-responsive and high-capacity adsorbents for wastewater treatment [8,9].

With the development of polymeric hydrogels, the incorporation of polysaccharides such as starch [11–13], cellulose [14,15], or chitosan [4,16] into the hydrogel structure has been considered. Starch is a renewable, abundant, low-cost, and fully biodegradable natural material that suffers from some drawbacks such as poor mechanical properties and poor long-term stability intensified by water absorption [17]. In order to overcome these issues, various physical or chemical modifications have been considered. Graft copolymerization of starch with hydrophilic monomers resulted in corresponding hydrogels with proper long-term stability and mechanical properties besides inexpensiveness, biodegradability, biocompatibility, and high swell-ability [11,13,16–18].

Recently, considerable interests have been generated for developing inexpensive adsorbents based on waste materials [19,20]. Eggshell (ES) is discarded as a waste material in large quantity by food manufacturers and restaurants. It weighs approximately 10% of the total mass (~60 g) of hen egg [21]. The main component (~90%) of ES is calcium carbonate ($CaCO_3$) [21]. The ES membrane is composed of a fibrous protein network that has a large surface area [22]. Many investigations have shown that ES is able to effectively adsorb metal ions [23,24], dyestuffs [22,25,26], and organic compounds [27]. The combination of ES particles as filler with polymeric hydrogels can provide cost-effective adsorbents with improved adsorption capacity. However, only a few articles were published on the polymeric hydrogel/ES particle composites as water pollutants adsorbent. Elkady [28] immobilized ES particles in alginate/poly(vinyl alcohol) hydrogel and used it as a biocomposite adsorbent for the removal of C.I. Remazol Reactive Red 198. More recently, we prepared chitosan-coated eggshell particles and employed it as a copper(II) biosorbent [29].

In this study, wheat starch was graft copolymerized with sodium methacrylate (NaMA) in the presence of different contents of ES particles with various size ranges to obtain hydrogel composites. The chemical structure, morphological properties, and water absorption of hydrogel composites were studied. Moreover, their ability to adsorb methylene blue (MB) and crystal violate (CV) as model basic (cationic) dyes was evaluated.

2. Experimental

2.1. Materials

All reagents including sodium methacrylate (NaMA) as hydrophilic monomer, N,N´-methylenebisacrylamide (MBA) as cross-linking agent, and ammonium persulfate (APS) as thermal initiator were purchased from Sigma-Aldrich and used as received. Wheat starch was bought from a local market. Hen eggshells were collected from a local restaurant, washed with hot distilled water, and dried at 70°C in a hot air oven for 4 h. Dried ES was grounded into powder using a grinder and sieved into size ranges of <75 μm, 75–150 μm, and 150–212 μm named as ES1, ES2, and ES3, respectively. The sieved ES particles were used without further chemical or physical treatment. Acetonitrile and acetone were bought from Merck and used as solvents during the preparation of hydrogel composites. Sodium hydroxide (NaOH), potassium dihydrogen phosphate (KH_2PO_4), and hydrochloride (HCl) from Merck were used for preparing phosphate-buffered saline (PBS). MB and CV used as model basic dyes were all of analytical grades.

2.2. Preparation of hydrogel composites

The free-radical graft copolymerization was used for preparing of hydrogel composites. A general procedure was as follows. Starch (3.0 g), NaMA (3.8 g), and MBA (1.0 g) were dissolved in 50 mL of distilled water/acetonitrile mixture (4/1, v/v). Desired amount of ES particles was added to the solution and the mixture was partially degassed through placing in an ultrasonic bath for 8 min to remove the dissolved oxygen. The reaction mixture was then transferred to a glass reactor equipped with a mechanical stirrer and a water bath preset at 75°C. Afterwards, APS (0.6 g) was added to the reactor. The gelation was observed after about 20–30 min. The formulations for the preparation of hydrogel composites are given in Table 1. To remove the unreacted reagents and also the prepared homopolymers (PNaMA), the prepared samples were washed three times with distilled water and then kept in 100 mL of acetone for 1 h in order to complete dehydration. Finally, hydrogel composites were dried at 40°C in a vacuum oven for 6 h and stored away from moisture and heat before use.

2.3. Instruments

The Fourier transformed infrared (FTIR) spectroscopy was accomplished using a Bruker

Table 1
Formulations of hydrogel composites

Sample code	Filler type	Filler particle size (μm)	Filler amount (g)	Gel content (%)
B1	–	–	0.0	99.6
B2	ES1	<75	2.8	99.7
B3	ES2	75–150	2.8	99.6
B4	ES3	150–212	2.8	99.7
B5	ES1	<75	1.4	99.6
B6	ES1	<75	4.2	99.7
B7	$CaCO_3$	<75	2.8	99.5

Notes: Bath temperature 75°C. For all samples: starch 3.0 g, NaMA 3.0 g, MBA 1.0 g, APS 0.6 g, and distilled water/acetonitrile mixture (4/1 v/v) 50 mL.

spectrophotometer (model Equinox 55, Germany) in the range of 400–4,000 cm^{-1} at 4 cm^{-1} resolution and 16 scans at room temperature. The morphology of samples was evaluated using field emission scanning electron microscopy (FE-SEM, model Mira, Tescan, Czech). Each sample was fixed on an aluminum pin using double-sided adhesive tape and then sputter coated with a thin gold layer for 4 min prior to examination. Optical microscopy was carried out using an Optika instrument (model B-180, Italy). UV–visible spectrometry was carried out using a Biochrom spectrophotometer (model WPA S2000 Lightwave, UK) at 664 and 580 nm for MB and CV, respectively, at ambient temperature. Distilled water was chosen as the blank. The concentrations of dyes were calculated using a five-point calibration curves obtained for each dye.

2.4. Measurements

To measure the gel content of the hydrogel composites, each of the samples (~0.05 g) was washed through immersing in plenty of distilled water for 3 d to completely extract the sol part. During this period, the washing medium was refreshed every 12 h. Then, the washed sample was dried at 90°C in a hot air oven for 6 h. The dried sample was then accurately weighed and the gel content values were calculated according to the following equation:

$$\text{Gel content } (\%) = (W_1/W_0) \times 100 \quad (1)$$

where W_0 and W_1 are the weights of unwashed (initial) and washed sample, respectively.

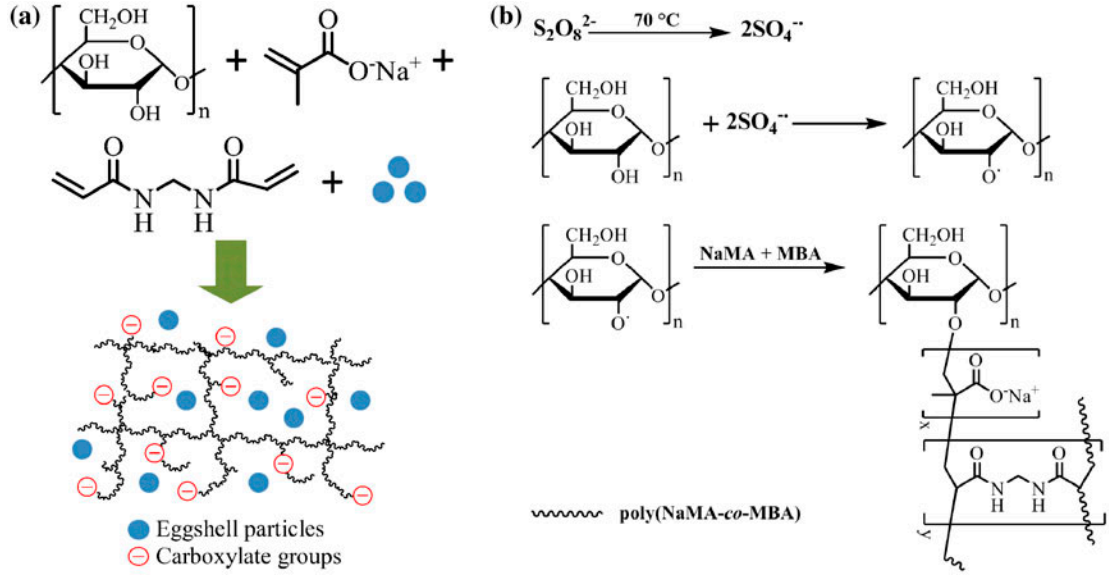

Fig. 1. (a) Preparation of hydrogel composites based starch-*g*-PNaMA/ES particles and (b) general graft copolymerization mechanism for the preparation of starch-*g*-PNaMA.

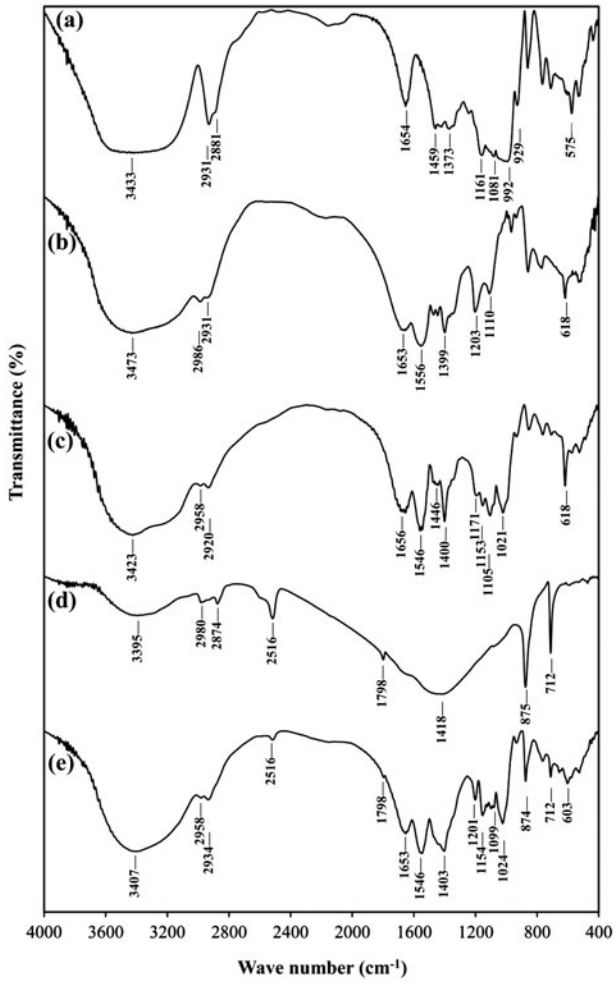

Fig. 2. FTIR spectra of starch (a), cross-linked PNaMA (b), sample B1 (c), ES (d), and sample B2 (e).

For determining the water absorption of the hydrogel composites, samples were completely dried at 40°C in a vacuum oven, accurately weighed (~0.05 g), and immersed in distilled water or PBS. After desired intervals, samples were removed from the media; their surface water was blotted using filter paper and weighed accurately. Water absorption values (WA) were calculated using the following equation:

$$\text{WA (g/g)} = [(W_1/W_0)/W_0] \quad (2)$$

where W_0 and W_1 are the weights of dried (initial) and swollen sample, respectively. The reported values are an average of three measurements.

To measure the dye adsorption of the hydrogel composites and ES particles, each sample (50 mg) was placed into a flask containing 10 mL aqueous solutions of MB and CV with concentration of 10 ppm (pH 5.5). The mixtures were shaken by a rotary shaker at room temperature. After desired intervals, the flasks were centrifuged at 4,000 rpm for 2 min to precipitate the adsorbents. Then, the concentration of remained dye in the solutions was determined using UV–visible spectrophotometer. The dye adsorption capacity (q) expressing the milligram of the adsorbed dye per gram of the adsorbent as well as dye removal (RE) were calculated using the following equations:

$$q\ (\text{mg/g}) = (C_0 - C_t) \times V/m \quad (3)$$

$$\text{RE}\ (\%) = (C_0 - C_t) \times 100/C_0 \quad (4)$$

where C_0 is the initial concentration of dye in the solution (in mg/L), C_t is the concentration of dye in the solution after contacting with the adsorbent for time t (in mg/L), V is the volume of the dye solution (in L), and m is the mass of the adsorbent (in g). The reported values are an average of three measurements.

3. Results and discussion

3.1. Synthesis and characterization of hydrogel composites

In this study, starch was modified through graft copolymerization with NaMA in the aqueous medium using MBA as cross-linking agent and APS as free-radical initiator to provide a cross-linked hydrogel containing carboxylate (COO^-) functions suitable for adsorbing basic dyes (Fig. 1(a)). Graft copolymerization of methacrylic acid (MAA) onto the glucose units of starch has been previously reported [17,18,30,31]. A general graft copolymerization mechanism for preparing starch-*g*-PNaMA is proposed in Fig. 1(b). While heating, APS is decomposed to produce sulfate anion radicals. These anion radicals abstract hydrogen atom from hydroxyl groups present on the starch backbone to form macro-radicals. Afterwards, these macro-radicals initiate the grafting copolymerization of NaMA and MBA on the starch backbone, yielding a three-dimensional structured graft copolymer [18].

Using a thermal initiator (APS) and a hydrophilic monomer (NaMA) makes homopolymer formation unavoidable during graft copolymerization. However, the gel content values were high (>99%, Table 1), which showed a good graft efficiency for the prepared hydrogels. This is due to using relatively high amounts of cross-linker (MBA) that bind a lot of PNaMA moieties into the hydrogel network as well as washing procedure that removed the ungrafted homopolymers (PNaMA).

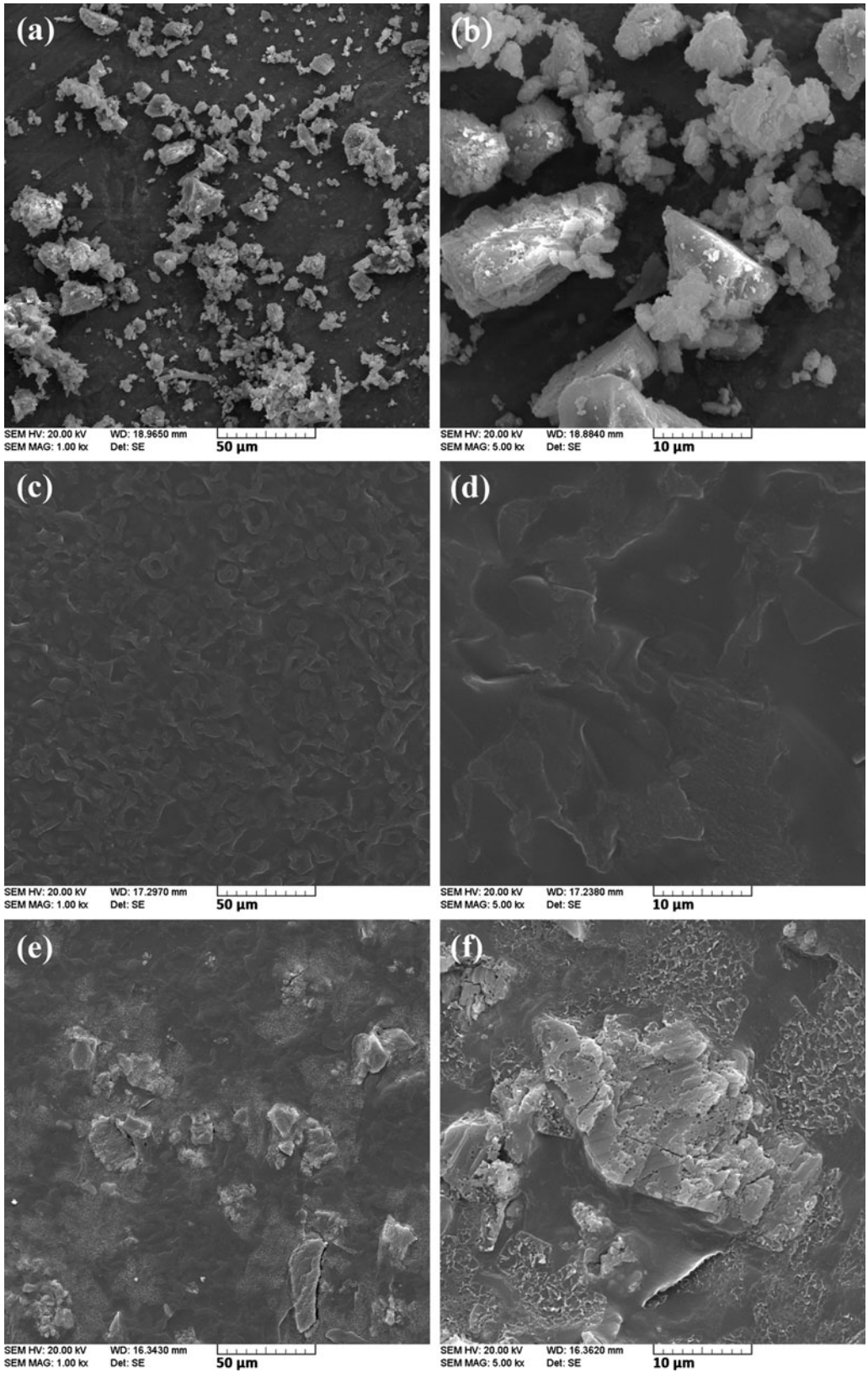

Fig. 3. SEM images of ES1 particles (a,b), samples B1 (c,d), and B2 (e,f).

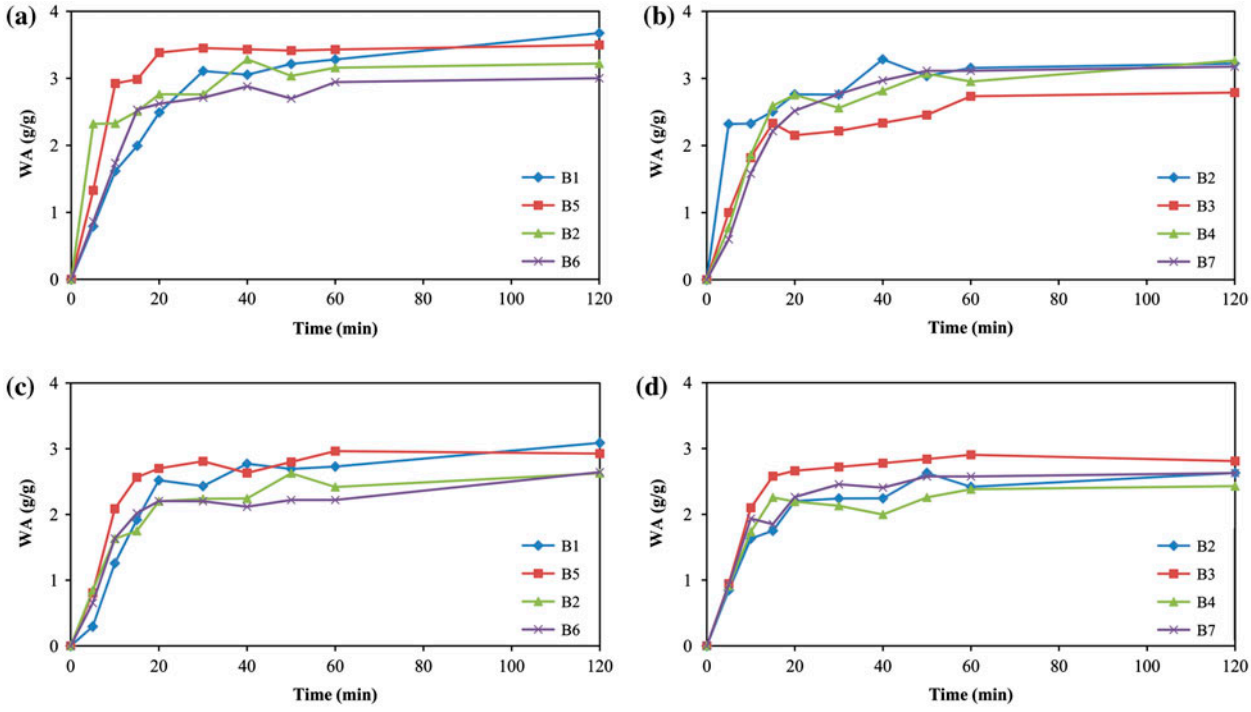

Fig. 4. Swelling of hydrogel composites vs. time in distilled water (a,b) and PBS (c,d) media. All experiments were performed at sample dose: 5 g/L and 25°C.

FTIR spectroscopy was employed to study the graft copolymerization reaction of NaMA and MBA onto starch backbone. FTIR spectra of starch, a cross-linked PNaMA (PNaMA-*co*-PMBA), and starch-*g*-PNaMA (sample B1) are given in Fig. 2(a)–(c). The FTIR spectrum of starch (Fig. 2(a)) showed the peaks related to stretching vibration of hydroxyl (O–H, a broad peak at 3,200–3,600 cm^{-1}), asymmetric stretching (2,931 and 2,881 cm^{-1}), and bending vibrations (1,459 cm^{-1}) of methylene (–CH_2–), and stretching vibrations of C–O bonds belong to ether (C–O–C, 1,161 cm^{-1}) and primary hydroxyl (C–OH, 1,081 cm^{-1}) groups [12,18]. The peak at 1,654 cm^{-1} is characteristic for starch [18]. Several opinions exist about the origin of this peak; the first overtone of bending vibration of hydroxyl groups [32], stretching vibration of ether groups [33], and angular bending vibration of O–H bond of absorbed water molecules [34,35]. FTIR spectrum of cross-linked PNaMA (Fig. 2(b)) showed the peaks related to the stretching vibration of carbonyl bond (C=O, 1,653 cm^{-1}) in amide moieties, asymmetric (1,556 cm^{-1}), and symmetric (1,399 cm^{-1}) stretching vibrations of carbonyl bond and the stretching vibration of C–O (1,203 cm^{-1}) bond of carboxylate groups (COO^-) [12,17]. According to Fig. 2(c), broad peak of starch hydroxyl groups (3,200–3,600 cm^{-1}) gets weakened in the sample B1 (3,423 cm^{-1}), implying that these groups have taken part in the graft copolymerization reaction [18,30]. The occurrence of starch corresponding peaks (1,446, 1,153, and 1,021 cm^{-1}) besides the peaks related to cross-linked PNaMA (1,656, 1,546, 1,400, 1,171, and 1,105 cm^{-1}) proved the successful synthesis of starch-*g*-PNaMA hydrogels [17,18,30]. Moreover, the absence of peaks related to the stretching vibration of =C–H bond (3,050 cm^{-1}) and the bending vibration (out of paper) of C=C bond (954 cm^{-1}) showed full consumption of vinyl groups during the graft copolymerization reaction.

To prepare hydrogel composites, the graft copolymerization reaction was carried out in the presence of different contents of ES particles (Fig. 1(a)). The separation of ES membrane is labor-intensive and time-consuming, thus the membrane-attached ES particles were used in this study. The combination of ES particles with the hydrogel matrix was also studied through FTIR spectroscopy. FTIR spectra of ES and sample B2 are given in Fig. 2(d)–(e). FTIR spectrum of ES (Fig. 2(d)) showed typical peaks of calcium carbonate (2,516, 1,798, 1,418, 875, and 712) as the main component of ES particles. The peaks at 1,418, 875, and 712 are, respectively, related to asymmetric stretching (v3) plus in-plane and out-of-plane bending vibrations of carbonate moieties [22,36]. The occurrence of these peaks in the FTIR spectrum of hydrogel

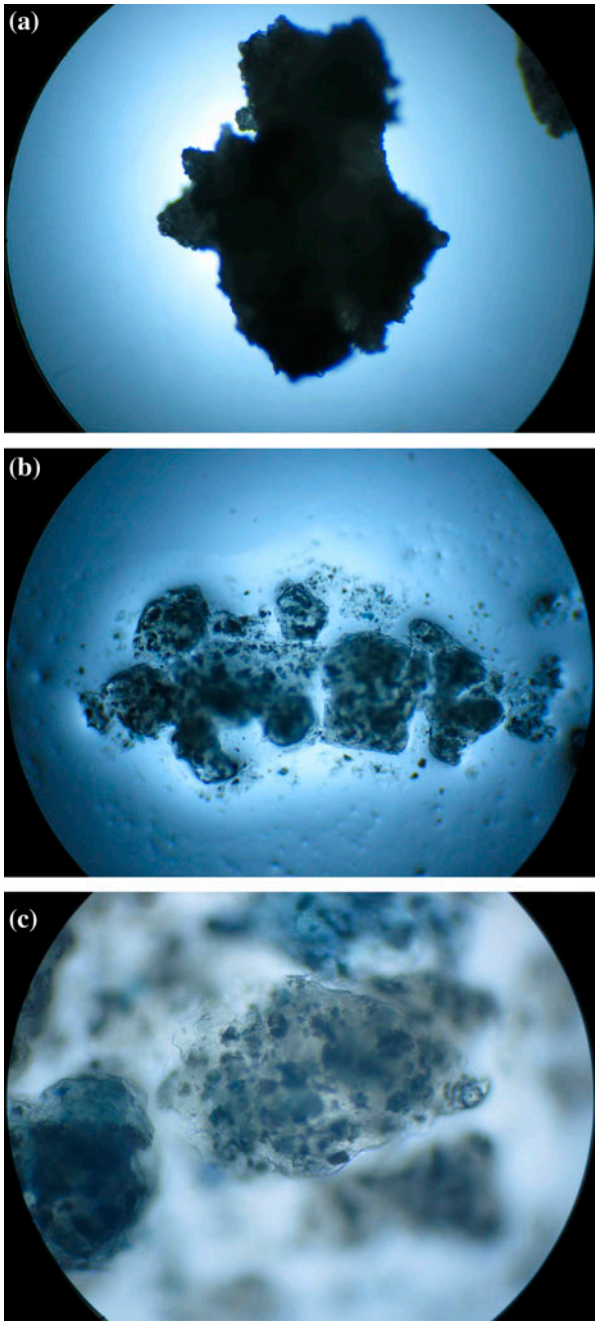

Fig. 5. Optical microscopy of sample B2 before (a) and after (b,c) swelling in distilled water for 24 h. Magnifications are ×40 (a,b) and ×100 (c).

composite (sample B2, Fig. 2(e)) confirmed the combination of ES particle into hydrogel matrix.

3.2. Morphological properties of hydrogel composites

Microstructure morphology is one of the most important properties that must be considered in adsorbents. SEM was used for studying the surface morphology of the prepared samples. Fig. 3 shows the SEM images of ES1 particles and samples B1 and B2. It can be clearly seen that the size of ES1 particles is in the range of 1–50 μm (Fig. 3(a)–(b)). ES1 particles exhibited an angular pattern of fractures due to their crystalline structure [22]. Moreover, surface structure of ES1 particles is rough, irregular, and porous. Roughness and porosity of surface can increase the available surface area for the adsorbtion of dye molecules.

According to SEM images, unfilled hydrogel (sample B1, Fig. 3(c)–(d)) showed a smooth surface with micro-scale phase separation due to the incompatibility of starch and PNaMA phases. This observation is in agreement with the previously reported results [18]. It is worth to be mentioned that the incompatibility was observed in spite of high cross-linking density of the prepared hydrogel. Hydrogel composite (sample B2, Fig. 3(e)–(f)) demonstrated good level of distribution for ES particles in the hydrogel matrix. Addition of ES particles into starch-*g*-PNaMA matrix increased the surface irregularity. Unexpectedly, incorporation of ES particles did not change the porosity of the hydrogel matrix, which can be related to its high cross-linking density. Moreover, ES particles incorporation did not affect the micro-scale phase separation into the starch-*g*-PNaMA matrix.

3.3. Water absorption of hydrogel composites

Water absorption profile of hydrogel composites was studied for distilled water and PBS media. Results are illustrated in Fig. 4. All samples showed fast water absorption in both media which reached equilibrium within ~30 min. The equilibrium water absorption of all samples was lower for PBS solution (2.43–3.09 g/g) compared to distilled water (2.79–3.68 g/g). This observation has been reported previously [37,38] and can be explained based on Flory theory [39]. In accordance with this theory, the water absorption of hydrogels decreases with an increase in the ionic strength of external solution. This decrease in water absorption could be attributed to the reduction in the osmotic pressure difference between the swollen hydrogel and the external solution [37].

According to Fig. 4(a) and (c), addition of ES particles into the starch-*g*-PNaMa matrix improved the water absorption rate at initial stage. In fact, ES particles facilitate the water absorption by reducing the transport resistance. However, the water absorption rate of hydrogel composites decreased at high contents of ES particles (samples B6). This trend was expected

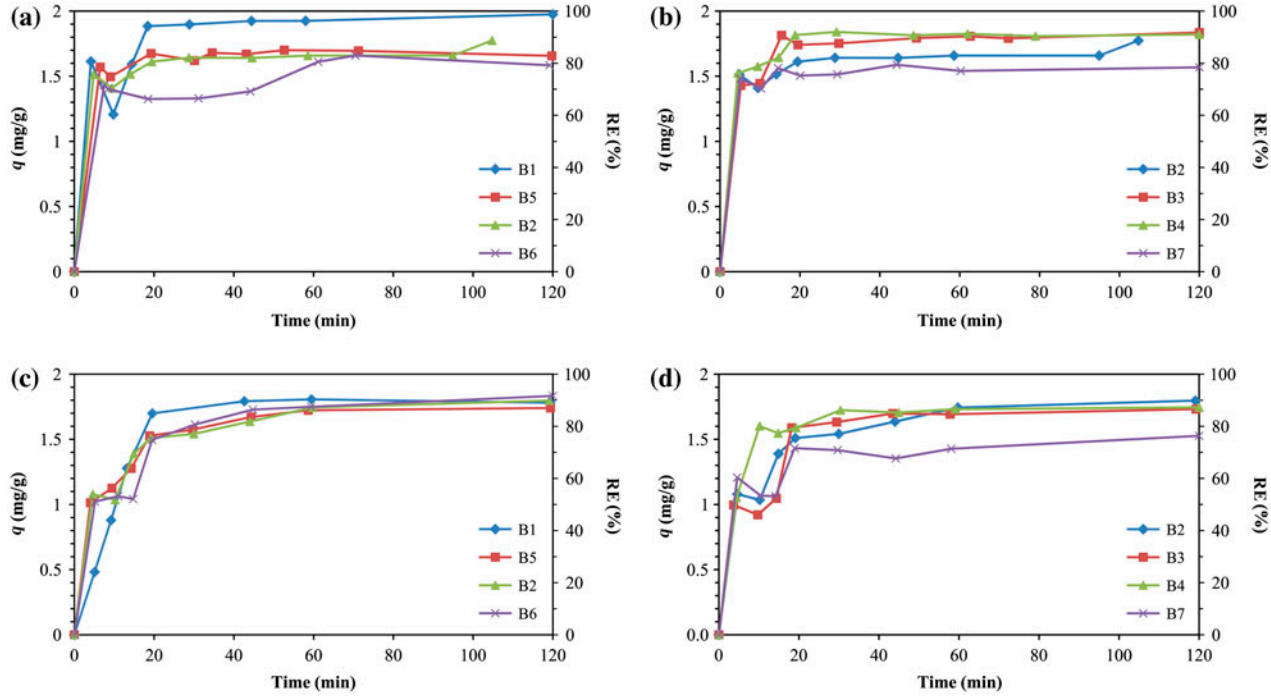

Fig. 6. Adsorption of MB (a,b) and CV (c,d) by hydrogel composites vs. time. All experiments were performed at sample dose: 5 g/L, dye initial concentration: 10 mg/L, pH 5.5, and 25°C.

on account of inability of ES particles to absorb water molecules. Due to this reason, the equilibrium WA values were lower for hydrogel composites with higher contents of ES particles (Fig. 4(a) and (c)). The morphological changes of hydrogel composites during water absorption were further investigated using optical microscopy. Fig. 5 shows the optical microscopic images of sample B2 before and after swelling in distilled water. According to Fig. 5, during the water absorption of sample B2, the starch-*g*-PNaMA matrix was swollen, while ES particles remained intact in the enlarged matrix. It is also worth to be mentioned that no sign of ES particles separation was observed after water absorption, which showed sufficient mechanical strength of swollen hydrogel composites.

The size range of ES particles was expected to be effective on the water absorption of corresponding hydrogel composites. In fact, the size range of ES particles can affect the pores and cavities in hydrogel structure. However, since the incorporated ES particles into hydrogel matrix did not affect their porosity, no specific trend of water absorption of hydrogels was observed relating to the size range of used ES particles. In distilled water medium, sample B2 containing ES1 particles (<75 μm) showed faster water absorption at initial stage, while the equilibrium water absorption had no significant trend related to size range of ES particles (Fig. 4(b)). On the contrary, in PBS medium, sample B3 based on ES2 particles (75–150 μm) showed higher water absorption at either initial stage or equilibrium condition (Fig. 4(d)). Moreover, no difference was observed for water absorbency of hydrogel composite based on ES particles (sample B2) and that based on calcium carbonate particles (sample B7), except sample B2 that showed faster water absorption at initial stage. This phenomenon indicated that the rough, irregular, and porous surface structure of ES particles had no significant influence on the water absorption of the starch-*g*-PNaMA matrix.

3.4. Dye adsorption of hydrogel composites

The dye adsorption profile of the hydrogel composites is represented in Fig. 6. The results showed that the equilibrium time for dye adsorption is lower than 30 min, indicating a fast adsorption for hydrogel composites. The equilibrium adsorption capacities for MB and CV were found to be in the range of 1.60–1.95 mg/g (removal of 80–97%) and 1.87–1.91 mg/g (removal of 94–96%), respectively. The main mechanisms of dye adsorption are electrostatic attraction between positively charged cationic moieties on the dye molecules and negatively charged carboxylate groups on the starch-*g*-PNaMA matrix as well as

Table 2
Kinetic parameters for dye adsorption of hydrogel composite

	MB							CV						
		PFO kinetic model			PSO kinetics model				PFO kinetic model			PSO kinetics model		
Samples code	$q_{e,exp}$ (mg/g)	R^2	$q_{e,cal}$ (mg/g)	k_1 (1/min)	R^2	$q_{e,cal}$ (mg/g)	k_2 (g/mg min)	$q_{e,exp}$ (mg/g)	R^2	$q_{e,cal}$ (mg/g)	k_1 (1/min)	R^2	$q_{e,cal}$ (mg/g)	k_2 (g/mg min)
B1	1.95 ± 0.01	0.640	0.861	8.53×10^{-2}	0.985	1.99	2.88×10^{-1}	1.88 ± 0.01	0.961	2.30	1.24×10^{-1}	0.952	2.34	3.63×10^{-2}
B2	1.64 ± 0.01	0.747	0.396	3.80×10^{-2}	0.996	1.71	4.32×10^{-1}	1.91 ± 0.01	0.819	0.932	4.76×10^{-2}	0.999	1.68	2.23×10^{-1}
B3	1.68 ± 0.04	0.291	0.376	7.09×10^{-2}	0.991	1.88	2.94×10^{-1}	1.88 ± 0.03	0.767	1.42	9.13×10^{-2}	0.982	1.05	1.64
B4	1.76 ± 0.02	0.665	0.597	2.44×10^{-1}	0.996	1.95	2.79×10^{-1}	1.87 ± 0.01	0.868	0.945	1.18×10^{-1}	0.995	1.88	1.81×10^{-1}
B5	1.60 ± 0.04	0.251	0.164	4.54×10^{-2}	0.998	1.66	1.13	1.87 ± 0.03	0.906	0.988	6.58×10^{-2}	0.984	1.80	1.25×10^{-1}
B6	1.65 ± 0.02	0.811	0.393	7.40×10^{-3}	0.999	1.38	1.97	1.89 ± 0.03	0.850	1.33	5.88×10^{-2}	0.971	1.94	8.00×10^{-2}
B7	1.61 ± 0.01	0.026	0.063	2.19×10^{-2}	0.998	1.53	2.00	1.89 ± 0.02	0.536	0.596	5.99×10^{-2}	0.980	1.53	2.80×10^{-1}

Notes: All experiments were performed at sample dose: 5 g/L, dye initial concentration: 10 mg/L, pH 5.5, contact time: 2 h and 25°C.

Table 3
Comparison of the kinetics parameters for dye adsorption of various adsorbents

Adsorbent	Dye	Adsorption condition (dosage, dye concent., pH, temp.)	$q_{e,exp}$ (mg/g)	Kinetic model	$q_{e,cal}$ (mg/g)	k_2 (g/mg min)	Refs.
Activated carbon	MB	0.025 g/L, 8 ppm, 5, 30°C	295	PSO	309	1.77×10^{-5}	[44]
Activated carbon treated with HCl	MB	0.025 g/L, 8 ppm, 5, 30°C	270	PSO	282	1.90×10^{-5}	[44]
Activated carbon treated with HNO_3	MB	0.025 g/L, 8 ppm, 5, 30°C	275	PSO	272	2.05×10^{-5}	[44]
Sepiolite	Methyl violet	2.5 g/L, 490 ppm, 5, 30°C	68.1	PSO	68.3	3.32×10^{-3}	[45]
Sepiolite	MB	2.5 g/L, 384 ppm, 5, 30°C	56.9	PSO	58.2	3.63×10^{-3}	[45]
ES particles (15 μm)	Acid orange 51	0.25 g/L, 10 ppm, 7, 25°C		PSO	28.7	1.60×10^{-2}	[40]
ES particles (<250 μm)	Malachite green	2 g/L, 50 ppm, 9, 25°C	52.4	PSO	52.7	8.9×10^{-4}	[26]
ES particles (<75 μm)	MB	5 g/L, 10 ppm, 5.5, 25°C	0.53	PFO	0.497	6.40×10^{-1}	[46]
ES particles (<75 μm)	CV	5 g/L, 10 ppm, 5.5, 25°C	1.72	PFO	1.38	7.69×10^{-1}	[46]
Poly(AA-AAm-MMA)/amylose semi-IPN hydrogels	CV	0.5 g/L, 10 ppm, 7.4, 25°C	28.6	PFO	27.6	3.5×10^{-4}	[8]
Chitosan-*g*-PAA/vermiculite hydrogel composites	MB	5 g/L, 1,000 ppm, 7, 30°C	1,684	PFO	1,691	5.74×10^{-4}	[47]
Alginate/PVAl/ES particles biocomposite	Reactive red	10 g/L, 10 ppm, 1, 22°C	0.98	PFO	1.1	3.66×10^{-2}	[28]
Starch-*g*-PNaMA/ES particles hydrogel composite	MB	5 g/L, 10 ppm, 5.5, 25°C	1.65	PFO	1.38	1.97	This work
Starch-*g*-PNaMA/ES particles hydrogel composite	CV	5 g/L, 10 ppm, 5.5, 25°C	1.89	PFO	1.94	8.00×10^{-2}	This work

hydrophobic interactions between dye molecules and hydrogel [8]. ES particles within the hydrogel matrix can also adsorb the dye molecules due to their porous structures and surface charge [22,27]. According to Fig. 6(a), addition of ES particles within the hydrogel matrix slightly decreased the MB adsorption capacity, which was expected due to low adsorbability of ES particles for MB [22,40]. Addition 60% low-cost ES particles into the starch-*g*-PNaMA matrix provided cost-effective hydrogel composite with slightly lower MB removal (from 97 to 89%). Moreover, hydrogel composites showed faster CV adsorption at initial stage and same equilibrium adsorption capacity in comparison with unfilled hydrogel (Fig. 6(c) and Table 2).

According to Fig. 6(b) and (d), the size range of ES particles within the hydrogel composites was effective on their dye adsorption rate. Hydrogel composite based on larger ES particles (samples B4) showed higher dye adsorption rate at initial stage compared with the smaller ones (samples B2 and B3). However, all filled samples had same equilibrium dye adsorption capacity, regardless of the size of ES particles. Pure ES particles had also the same equilibrium dye adsorption values, regardless of their size (data not shown). Moreover, hydrogel composites based on ES particles showed higher dye adsorption rate and capacity compared to those based on calcium carbonate (sample B7) due to rougher and more irregular porous structure of ES particles surface (Fig. 6(b) and (d)).

In order to investigate the kinetic mechanism of dye adsorption by hydrogel composites, the experimental data were analyzed according to linear forms of pseudo-first-order (PFO) and pseudo-second-order (PSO) kinetic models. The linear forms of PFO and

PSO models can be expressed according to the following equations [41,42]:

$$\ln\,(q_e - q_t) = \ln\,q_e - k_1 t \tag{5}$$

$$\frac{t}{q_t} = \frac{t}{q_e} + \frac{1}{k_2 q_e^2} \tag{6}$$

where q_t (mg/g) is the amount of adsorbed dye molecules at time t (min), and k_1 (1/min) and k_2 (g/mg min) are, respectively, the rate constants of PFO and PSO adsorptions. For PFO model, the values of k_1 and q_e were obtained from the slope and intercept of $\ln\,(q_e - q_t)$ vs. t plot, respectively. For PSO model, the slope and intercept of t/q_t vs. t plot showed, respectively, q_e and k_2 values.

The results for the kinetic models are given in Table 2. The regression correlation coefficient (R^2) values were reported to indicate the goodness of the kinetic model fit. For all samples, higher R^2 value was obtained with the PSO model compared to the PFO model (Table 2). Moreover, the calculated equilibrium adsorption capacities ($q_{e,cal}$) obtained from the PSO model were well approximated to the experimental ones ($q_{e,exp}$) indicating better suitability of this model to describe dye adsorption kinetics onto hydrogel composites [26]. Therefore, the rate-controlling step for the overall sorption processes is chemisorption involving are electrostatic attraction between positively charged cationic moieties on the dye molecules and negatively charged carboxylate groups on the PNaMA matrix [8,43]. Previous study has also reported that the adsorption of CV on semi-interpenetrated network hydrogels constituted of poly(acrylic acid-acrylamide-methacrylate) and amylose followed the PSO kinetics [8]. Moreover, the adsorption of acid orange 51 [40] and malachite Green [26] on ES particles followed the PSO kinetics.

As expected, the incorporation of ES particles results in higher k_2 and lower $q_{e,cal}$ values for hydrogel composites. Moreover, samples based on larger ES particles (samples B3 and B4) showed lower k_2 and higher $q_{e,cal}$ values.

The equilibrium adsorption capacities and kinetics parameters for dye adsorption of sample B6 are compared with those for other adsorbents in Table 3. Sample B6 exhibits proper equilibrium adsorption capacity and kinetics compared to other adsorbents with similar adsorption conditions. Considering the utilization of 60% ES particles as a waste matrix within sample B6, our developed biosorbent can be used as a cost-effective adsorbent for water purification.

4. Conclusions

Eggshell (ES) particles as an available and low-cost waste material were incorporated into starch-*g*-PNaMA to prepare hydrogel composites as dye biosorbents. FTIR spectroscopy confirmed the grafting of PNaMA moieties onto starch backbone as well as combination of ES particles with the hydrogel composites. The gel content values were high (>99%) which showed proper graft efficiency for the prepared hydrogel composites. SEM images demonstrated good level of distribution for ES particles in the hydrogel matrix. Addition of ES particles into starch-*g*-PNaMA matrix resulted in higher water absorption rate at initial stage due to higher porosity, while the equilibrium water absorption was decreased. Incorporation of ES particles into hydrogel matrix resulted in faster water absorption at initial stage and lower equilibrium water absorption capacity. Addition of 60% low-cost ES particles into starch-*g*-PNaMA provided a cost-effective adsorbent with similar CV adsorption capacity compared to unfilled hydrogel, while MB removal was slightly decreased. The dye adsorption by hydrogel composites followed the pseudo-second-order kinetics indicating that chemical sorption is the rate-limiting step.

References

[1] F. Fu, Q. Wang, Removal of heavy metal ions from wastewaters: A review, J. Environ. Manage. 92 (2011) 407–418.
[2] N. Kannan, M.M. Sundaram, Kinetics and mechanism of removal of methylene blue by adsorption on various carbons-a comparative study, Dyes Pigm. 51 (2001) 25–40.
[3] M. Valix, W.H. Cheung, G. McKay, Preparation of activated carbon using low temperature carbonisation and physical activation of high ash raw bagasse for acid dye adsorption, Chemosphere 56 (2004) 493–501.
[4] G.L. Dotto, L.A.A. Pinto, Adsorption of food dyes onto chitosan: Optimization process and kinetic, Carbohydr. Polym. 84 (2011) 231–238.
[5] W.S.W. Ngah, L.C. Teong, M.A.K.M. Hanafiah, Adsorption of dyes and heavy metal ions by chitosan composites: A review, Carbohydr. Polym. 83 (2011) 1446–1456.
[6] M.F.A. Taleb, D.E. Hegazy, S.A. Ismail, Radiation synthesis, characterization and dye adsorption of alginate-organophilic montmorillonite nanocomposite, Carbohydr. Polym. 87 (2012) 2263–2269.
[7] A. Li, J. Zhang, A. Wang, Utilization of starch and clay for the preparation of superabsorbent composite, Bioresour. Technol. 98 (2007) 327–332.
[8] S. Li, Removal of crystal violet from aqueous solution by sorption into semi-interpenetrated networks hydrogels constituted of poly(acrylic acid-acrylamide-methacrylate) and amylose, Bioresour. Technol. 101 (2010) 2197–2202.

[9] V. Bekiari, M. Sotiropoulou, G. Bokias, P. Lianos, Use of poly(N,N-dimethylacrylamide-co-sodium acrylate) hydrogel to extract cationic dyes and metals from water, Colloids Surf., A 312 (2008) 214–218.
[10] H.Y. Zhu, Y.Q. Fu, R. Jiang, J. Yao, L. Xiao, G.M. Zeng, Novel magnetic chitosan/poly(vinyl alcohol) hydrogel beads: Preparation, characterization and application for adsorption of dye from aqueous solution, Bioresour. Technol. 105 (2012) 24–30.
[11] J.R. Witono, I.W. Noordergraaf, H.J. Heeres, L.P.B.M. Janssen, Graft copolymerization of acrylic acid to cassava starch—Evaluation of the influences of process parameters by an experimental design method, Carbohydr. Polym. 90 (2012) 1522–1529.
[12] S. Kiatkamjornwong, K. Mongkolsawat, M. Sonsuk, Synthesis and property characterization of cassava starch grafted poly[acrylamide-co-(maleic acid)] superabsorbent via γ-irradiation, Polymer 43 (2002) 3915–3924.
[13] V.D. Athawale, V. Lele, Graft copolymerization onto starch. II. Grafting of acrylic acid and preparation of it's hydrogels, Carbohydr. Polym. 35 (1998) 21–27.
[14] E.S. Abdel-Halim, S.S. Al-Deyab, Chemically modified cellulosic adsorbent for divalent cations removal from aqueous solutions, Carbohydr. Polym. 87 (2012) 1863–1868.
[15] C. Demitri, R.D. Sole, F. Scalera, A. Sannino, G. Vasapollo, A. Maffezzoli, L. Ambrosio, L. Nicolais, Novel superabsorbent cellulose-based hydrogels crosslinked with citric acid, J. Appl. Polym. Sci. 110 (2008) 2453–2460.
[16] Y. Zheng, D. Huang, A. Wang, Chitosan-g-poly(acrylic acid) hydrogel with crosslinked polymeric networks for Ni^{2+} recovery, Anal. Chim. Acta 687 (2011) 193–200.
[17] I. Silva, M. Gurruchaga, I. Goñi, Drug release from microstructured grafted starch monolithic tablets, Starch/Stärke 63 (2011) 808–819.
[18] V. Nikolic, S. Velickovic, A. Popovic, Amine activators influence on grafting reaction between methacrylic acid and starch, Carbohydr. Polym. 88 (2012) 1407–1413.
[19] J. Carvalho, J. Araujo, F. Castro, Alternative low-cost adsorbent for water and wastewater decontamination derived from eggshell waste: An overview, Waste Biomass Valorization 2 (2011) 157–167.
[20] V.K. Gupta, Suhas, Application of low-cost adsorbents for dye removal—A review, J. Environ. Manage. 90 (2009) 2313–2342.
[21] J. Kovacs-Nolan, M. Phillips, Y. Mine, Advances in the value of eggs and egg components for human health, J. Agric. Food. Chem. 53 (2005) 8421–8431.
[22] W.T. Tsai, J.M. Yang, C.W. Lai, Y.H. Cheng, C.C. Lin, C.W. Yeh, Characterization and adsorption properties of eggshells and eggshell membrane, Bioresour. Technol. 97 (2006) 488–493.
[23] S. Wang, M. Wei, Y. Huang, Biosorption of multifold toxic heavy metal ions from aqueous water onto food residue eggshell membrane functionalized with ammonium thioglycolate, J. Agric. Food. Chem. 61 (2013) 4988–4996.
[24] M. Ahmad, A.R.A. Usman, S.S. Lee, S.-C. Kim, J.-H. Joo, J.E. Yang, Y.S. Ok, Eggshell and coral wastes as low cost sorbents for the removal of Pb^{2+}, Cd^{2+} and Cu^{2+} from aqueous solutions, J. Ind. Eng. Chem. 18 (2012) 198–204.
[25] P.S. Guru, S. Dash, Adsorption of some tailor-made styrylpyridinium dyes on sodium dodecylsulphate-treated eggshell particles (SDS-ESP): Impact of dye chain-length and substituent, J. Dispersion Sci. Technol. 34 (2013) 898–907.
[26] S. Chowdhury, P. Das, Utilization of a domestic waste-Eggshells for removal of hazardous Malachite Green from aqueous solutions, Environ. Prog. Sustain. Energy 31 (2012) 415–425.
[27] B. Koumanova, P. Peeva, S.J. Allen, K.A. Gallagher, M.G. Healy, Biosorption from aqueous solutions by eggshell membranes and Rhizopus oryzae: equilibrium and kinetic studies, J. Chem. Technol. Biotechnol. 77 (2002) 539–545.
[28] M.F. Elkady, A.M. Ibrahim, M.M.A. El-Latif, Assessment of the adsorption kinetics, equilibrium and thermodynamic for the potential removal of reactive red dye using eggshell biocomposite beads, Desalination 278 (2011) 412–423.
[29] J. Mohammadnezhad, F. Khodabakhshi-Soreshjani, H. Bakhshi, Preparation and evaluation of chitosan-coated eggshell particles as copper(II) biosorbent, Desalin Water Treat. (2015), doi: 10.1080/19443994.2014.976276.
[30] B. Singh, D.K. Sharma, A. Gupta, In vitro release dynamics of thiram fungicide from starch and poly (methacrylic acid)-based hydrogels, J. Hazard. Mater. 154 (2008) 278–286.
[31] M.K. Beliakova, A.A. Aly, F.A. Abdel-Mohdy, Grafting of poly(methacrylic acid) on starch and poly(vinyl alcohol), Starch/Stärke 56 (2004) 407–412.
[32] S. Pal, D. Mal, R.P. Singh, Cationic starch: An effective flocculating agent, Carbohydr. Polym. 59 (2005) 417–423.
[33] E.J. Lee, D.K. Kweon, B.K. Koh, S.T. Lim, Physical characteristics of sweet potato pulp/polycaprolactone blends, J. Appl. Polym. Sci. 92 (2004) 861–866.
[34] C.P.B. Melo, M.V.E. Grossmann, F. Yamashita, E.Y. Youssef, L.H. Dall'Antonia, S. Mali, Effect of manufacturing process and xanthan gum addition on the properties of cassava starch films, J. Polym. Environ. 19 (2011) 739–749.
[35] D.C. Dragunski, A. Pawlicka, Preparation and characterization of starch grafted with toluene poly (propylene oxide) diisocyanate, Mater. Res. 4 (2001) 77–81.
[36] G. Busca, C. Resini, Vibrational spectroscopy for the analysis of geological and inorganic materials, in: R.A. Meyers (Ed.), Encyclopedia of Analytical Chemistry, John Wiley & Sons, Chichester, UK, 2000, pp. 10954–11008.
[37] S. Hua, A. Wang, Preparation and properties of superabsorbent containing starch and sodium humate, Polym. Adv. Technol. 19 (2008) 1009–1014.
[38] S.P. Bhuniya, S. Rahman, A.J. Satyanand, M.M. Gharia, A.M. Dave, Novel route to synthesis of allyl starch and biodegradable hydrogel by copolymerizing allyl-modified starch with methacrylic acid and acrylamide, J. Polym. Sci., Part A: Polym. Chem. 41 (2003) 1650–1658.
[39] P.J. Flory, Principle of Polymer Chemistry, Cornell University Press, New York, NY, 1953.

[40] W.T. Tsai, K.J. Hsien, H.C. Hsu, C.M. Lin, K.Y. Lin, C.H. Chiu, Utilization of ground eggshell waste as an adsorbent for the removal of dyes from aqueous \solution, Bioresour. Technol. 99 (2008) 1623–1629.
[41] W.S.W. Ngah, A. Kamari, Y.J. Koay, Equilibrium and kinetics studies of adsorption of copper (II) on chitosan and chitosan/PVA beads, Int. J. Biol. Macromol. 34 (2004) 155–161.
[42] F.C. Wu, R.L. Tseng, R.S. Juang, Kinetic modeling of liquid-phase adsorption of reactive dyes and metal ions on chitosan, Water Res. 35 (2001) 613–618.
[43] S.K. Bajpai, C. Navin, M. Manika, The adsorptive removal of cationic dye from aqueous solution using poly(methacrylic acid) hydrogels: Part-I. Equlibrium studies, Int. J. Environ. Sci. 2 (2012) 1609–1624.
[44] S. Wang, Z.H. Zhu, A. Coomes, F. Haghseresht, G.Q. Lu, The physical and surface chemical characteristics of activated carbons and the adsorption of methylene blue from wastewater, J. Colloid Interface Sci. 284 (2005) 440–446.
[45] M. Doğan, Y. Özdemir, M. Alkan, Adsorption kinetics and mechanism of cationic methyl violet and methylene blue dyes onto sepiolite, Dyes Pigm. 75 (2007) 701–713.
[46] A. Darvishi, H. Bakhshi, Poly(sodium methacrylate)/eggshell particle hydrogel composites as dye sorbent: Synthesis and characterization, Polym. Bull. (2015).
[47] Y. Liu, Y. Zheng, A. Wang, Enhanced adsorption of Methylene Blue from aqueous solution by chitosan-g-poly (acrylic acid)/vermiculite hydrogel composites, J. Environ. Sci. 22 (2010) 486–493.